Glass Film Structure of Grain-Oriented Silicon Steel Using Aluminum Nitride as an Inhibitor

H. Fujii, S. Yamazaki, T. Nagashima, H. Kobayashi, H. Masui, and M. Shiozaki

The composition and structure of glass (silicate) film formed during secondary recrystallization annealing of grain-oriented 3% Si steel using aluminum nitride as an inhibitor was investigated. The glass film consisted of spinel ($MgO \cdot Al_2O_3$) and forsterite [$2(MgO) \cdot SiO_2$], and the Al_2O_3 component of spinel originates from aluminum generated by the decomposition of aluminum nitride. From the location and the morphology of the spinel, it was concluded that aluminum reacts with forsterite to form spinel.

Keywords

aluminum concentration, aluminum nitride, characterization, forsterite, glass film structure, grain-oriented silicon steel, SEM/EPMA analysis, spinel, spinel formation mechanism, X-ray diffraction analysis

1. Introduction

GRAIN-ORIENTED silicon steel is covered with a glass (silicate) film. This film is produced by the reaction between silica (SiO_2) formed during decarburization annealing and magnesia (MgO) applied to the surface prior to secondary recrystallization annealing. It is industrially important to form the glass film uniformly and without defects in order to ensure the adhesion of a tension coating on the glass film and the electrical insulation of the surface. It is well accepted that the main component of the glass film is forsterite [$2(MgO) \cdot SiO_2$].

Previous studies (Ref 1, 2) have focused on the effects of the glass film on magnetic properties. Few investigations, however, have dealt with the structure of the glass film—especially the glass film (Ref 3) on silicon steel when aluminum nitride (AlN) is used as an inhibitor for the secondary recrystallization. The main objective of the present work was to characterize the glass film and its process of formation during secondary recrystallization annealing of 3% Si steel using AlN as an inhibitor. The composition, morphology, and elemental distributions in the glass film were studied.

2. Experimental Procedure

2.1 *Test Materials and Heat Treatment*

Sample preparation for characterization was as follows. Sheets of silicon steel (Fe-0.080C-3.28Si-0.074Mn-0.028Al-0.0255 → 0.025S) were cold rolled to a thickness of 0.26 mm. The cold-rolled sheets were annealed at 850 °C (1123 K) for 60 s in a $25N_2$-$75H_2$ atmosphere containing H_2O (H_2O/H_2 ratio of 0.44). Prior to secondary recrystallization annealing, an annealing separator composed mainly of a MgO slurry was applied to the surfaces. The cycle of the secondary recrystallization annealing consisted of a 15 °C/h heating rate from room temperature to a soak temperature of 1200 °C (1473 K) in a $25N_2$-$75H_2$ atmosphere, an isothermal soak for 20 h in 100% H_2, and cooling from the isothermal soak temperature to near room temperature. During this annealing, both secondary recrystallization and formation of the glass film occurred.

To investigate the effect of aluminum concentration on the glass film composition, sheets with various aluminum contents were cold rolled to a thickness of 0.225 mm. The contents of acid-soluble aluminum in the samples were 22, 201, 322, and 457 ppm. Sheets were annealed at 850 °C (1123 K) for 150 s in a $25N_2$-$75H_2$ atmosphere containing H_2O (H_2O/H_2 ratio of 0.44). These samples had a slurry of MgO applied to the surface and were annealed under the same conditions outlined above.

2.2 *X-ray Diffraction Analysis*

The glass films were extracted from the steel by the potentiostatic electrolysis method using a nonaqueous solution (at around –200 mV versus a saturated calomel electrode [SCE] in 10% acetylacetone plus 1% tetramethylammonium chloride-methanol) (Ref 4) and were collected by filtration from the solution using filters with a pore diameter of 0.2 μm.

2.3 *SEM/EPMA Analysis*

Before observing the morphology by scanning electron microscopy (SEM) and analyzing the element distribution by electron probe microanalysis (EPMA), samples polished in the cross section were etched by the potentiostatic electrolysis method using a nonaqueous solution (at 150 mV_{SCE} in 4 C for a sample size of 20 by 10 mm) (Ref 5). After drying and evaporation of carbon, the sample was examined by SEM/EPMA (Shimadzu™, Shimadzu Scientific Instruments, Inc., Columbia, MA, EPMA-8705).

2.4 *Chemical Analysis of Glass Film Composition (Ref 6)*

The glass films were extracted in the same manner previously described. After flux additions of $Na_2B_4O_7$, Na_2CO_3, and $CaCO_3$, the extracts were fused in platinum crucibles for vitrification. A homogeneous aqueous solution was prepared from the vitrified extracts with HCl and was quantitatively analyzed using the inductively coupled plasma method.

H. Fujii, S. Yamazaki, T. Nagashima, and **H. Masui,** Nippon Steel Corporation, Technical Development Bureau, Steel Research Laboratories, Electromagnetic Materials, Futtsu 299-12, Japan; **H. Kobayashi,** Nippon Steel Corporation, Technical Development Bureau, Advanced Materials & Technology, Materials Characterization, Kawasaki 211, Japan; **M. Shiozaki,** Nittech Research Corporation, Himeji 671-11, Japan

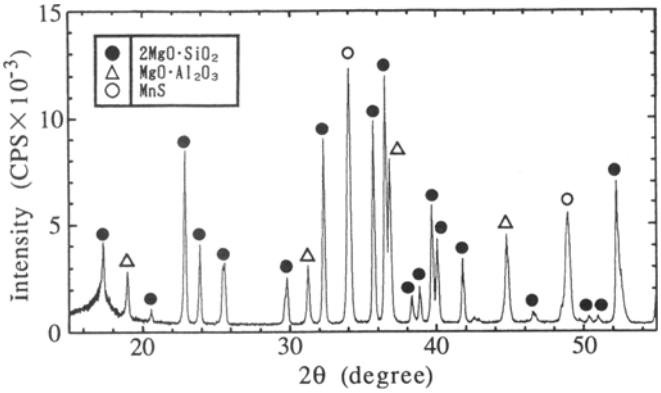

Fig. 1 X-ray diffraction pattern of the glass film extracted from 3% Si steel using AlN as an inhibitor to grain growth during secondary recrystallization (Cu K_α)

Table 1 Comparison between observed data and JCPDS of x-ray reflections of spinel(a)

hkl	d/Å (observed)	d/Å (JCPDS)
111	4.66	4.66
220	2.858	2.858
311	2.436	2.437
400	2.022	2.020
422	1.650	1.650
511	1.556	1.5554
440	1.429	1.4289

(a) Observed data were calibrated using forsterite reflections (the Joint Committee on Powder Diffraction Standards:34-189) as an internal standard.

3. Experimental Results

3.1 *X-ray Diffraction Analysis*

Figure 1 shows a typical x-ray diffraction pattern of the glass film extracted from a sample. The broad peak at around $2\theta = 15°$ is ascribed to the filter used for the extraction. Diffraction peaks identified with solid circles are ascribed to forsterite (Ref 7). Peaks identified with open circles are ascribed to manganese sulfide. In addition to these diffraction peaks, other peaks (open triangles) were observed. Comparison of these peaks with those of many compounds identified them as derived from spinel. Until now, there have been no reports of the existence of spinel in glass films. In order to confirm this identification, the observed reflection values were compared with standard values (Table 1). The observed values of the peaks supposedly derived from spinel were calibrated using the reflection peaks of forsterite as internal standards. The observed values were in good agreement with the standard values (Ref 8). Consequently, the newly observed reflection peaks have been identified as being derived from cubic-type spinel. From these results, it has been concluded that, in addition to forsterite, spinel is a constituent of the glass film.

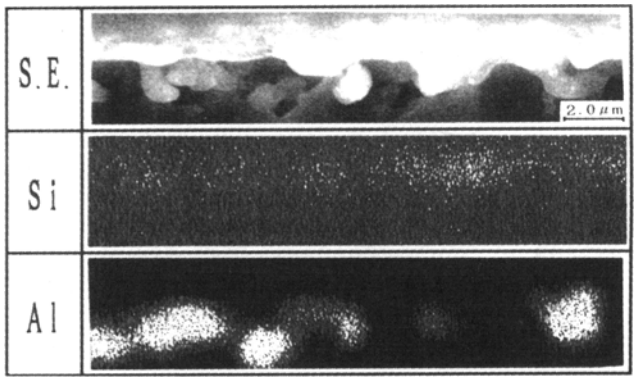

Fig. 2 Secondary electron image and characteristic x-ray images of cross sections of the glass film

3.2 *SEM/EPMA Analysis*

Figure 2 shows the secondary electron image observed by SEM and the characteristic x-ray images detected by EPMA of the cross section of the glass film. The secondary electron image shows that the glass film is composed of two parts: (1) a filmlike structure covering the surface and (2) particles or parts protruding from the filmlike structure. Color mapping of element distribution detected the characteristic x-ray of silicon from the filmlike structure and that of aluminum from protruding particles. Forsterite consists of magnesium, silicon, and oxygen; spinel consists of magnesium, aluminum, and oxygen. Therefore, the region in which silicon is detected is forsterite and the region in which aluminum is detected is spinel. It was concluded that the filmlike structure is forsterite and that the particles or the parts protruding from forsterite into the matrix are spinel.

3.3 *Influence of Aluminum Concentration on Glass Film Composition*

The molar ratio of aluminum to magnesium was calculated from the results of chemical analysis of the glass film. Figure 3 shows the influence of initial acid-soluble aluminum concentration on the composition of the glass film. The molar ratio of aluminum to magnesium in the glass film increases steadily with increasing acid-soluble aluminum concentration. X-ray diffraction analysis has shown that the aluminum component constitutes the spinel in the glass film. Accordingly, the results shown in Fig. 3 reveal that the amount of spinel in the glass film increases with increasing acid-soluble aluminum concentration.

4. Discussion

4.1 *Structure of the Glass Film*

The primary component of the glass film is forsterite, which consists of silica and magnesia. The origin of the MgO component of forsterite is magnesia powder applied to the surface prior to secondary recrystallization annealing. The origin of the SiO_2 component of forsterite is silica formed during decarburization annealing. Previous studies have shown that silica

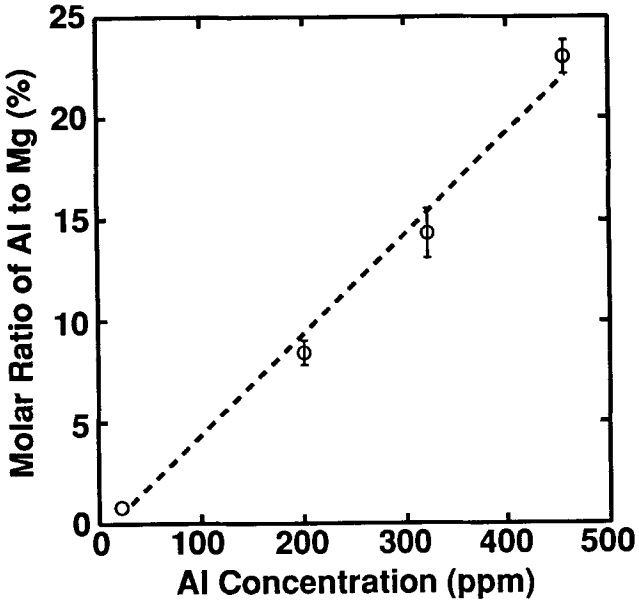

Fig. 3 Influence of initial acid-soluble aluminum concentration on the composition of the glass film

formed during decarburization annealing is amorphous (Ref 9). However, peaks in the region of low-diffraction angle were not observed in the x-ray diffraction pattern of the glass film (Fig. 1), which shows that an amorphous component does not exist in glass film. Also, an infrared spectrum of the glass film showed no peaks identified as silica. These results indicate that neither noncrystalline nor crystalline silica remains after secondary recrystallization annealing. Therefore, it can be concluded that silica formed during decarburization annealing is entirely consumed through the formation of the glass film.

X-ray diffraction analysis has shown that the glass film contains spinel in addition to forsterite. Spinel consists of magnesia and alumina. In both oxides, the MgO component is expected to originate from magnesia powder. On the basis of the results shown in Fig. 2, the origin of the Al_2O_3 component of spinel was considered. The molar ratio of aluminum to magnesium increases steadily with increasing acid-soluble aluminum concentration. Accordingly, the Al_2O_3 component contained in spinel originates from acid-soluble aluminum or AlN.

4.2 *Mechanism of Spinel Formation*

During secondary recrystallization annealing, AlN in steel decomposes to aluminum and nitrogen (Ref 10):

$$AlN \rightarrow Al + N \qquad \text{(Eq 1)}$$

As the secondary recrystallization starts from 950 °C (1223 K), it could be presumed that the reaction shown in Eq 1 starts from 950 °C (1223 K) (Ref 11). The decomposition of AlN causes aluminum to dissolve in the matrix. It could easily be expected that aluminum dissolved in the matrix begins to diffuse out to the surface. On the other hand, the reaction of forsterite formation on the surface remarkably proceeds from 950 °C (1223 K) (Ref 12):

$$2(MgO) + SiO_2 \rightarrow 2(MgO) \cdot SiO_2 \qquad \text{(Eq 2)}$$

Accordingly, it could be expected that aluminum comes into contact with forsterite. Therefore, it has been concluded that aluminum that diffuses to the surface and forsterite formed on the surface react with each other to form spinel:

$$2(MgO) \cdot SiO_2 + 4Al \rightarrow 2(MgO \cdot Al_2O_3) + Si \qquad \text{(Eq 3)}$$

These reaction schemes are consistent with the glass film structure. The location and the morphology of spinel—that is, spinel is protruded from the forsterite film into the matrix—support the mechanism that spinel is formed by the reaction between the forsterite film and aluminum diffused from the matrix.

5. Conclusions

- The glass film consists of forsterite and spinel when AlN is used as an inhibitor for the secondary recrystallization of 3% Si steel.
- Spinel in the glass film is located just under the forsterite film.
- Spinel in the glass film is formed by the reaction between the forsterite film and aluminum decomposed from AlN during secondary recrystallization annealing.

References

1. W.G. Morris, J.W. Shilling, D.R. Fecich, and P. Rao, Effect of Forsterite Coating on the Domain Structure of Grain-Oriented 3-Percent Si-Fe, *IEEE Trans. Magn.*, Vol 14 (No. 1), 1978, p 14-17
2. S.D. Washko and T.H. Shen, The Effect of Forsterite Coating on Magnetic Properties and Domain Structure of Grain Oriented 3% Si-Fe, *J. Appl. Phys.*, Vol 53 (No. 11), 1982, p 8296-8298
3. S. Taguchi and A. Sakakura, Characteristics of Magnetic Properties of Grain-Oriented Silicon Iron with High Permeability, *J. Appl. Phys.*, Vol 40 (No. 3), 1969, p 1539-1541
4. F. Kurosawa, I. Taguchi, and R. Matsumoto, Observation of Precipitates and Metallographic Grain Orientation in Steel by a Non-aqueous Electrolyte—Potentiostatic Etching Method, *J. Jpn. Inst. Met.*, Vol 43, 1979, p 1068-1077
5. F. Kurosawa, Analytical Study on the Fe/Ti Interface in Titanium-Clad Steels, *Surf. Interface Anal.*, Vol 12, 1988, p 203-210
6. M. Saeki, F. Kurosawa, and M. Matsuo, Micro and State Analysis as the Basis for Microalloying Techniques, *Trans. Iron Steel Inst. Jpn.*, Vol 26, 1986, p 1017-1035
7. Powder Diffraction File No. 34-189, JCPDS International Center for Diffraction Data, Swarthmore, PA, 1991
8. Powder Diffraction File No. 21-1152, JCPDS International Center for Diffraction Data, Swarthmore, PA, 1991

9. W.F. Block and N. Jayaraman, Reactions during Decarburization Annealing of Electrical Steel, *Mater. Sci. Technol.*, Vol 2, 1986, p 22-27

10. S. Taguchi and A. Sakakura, The Effect of AIN on Secondary Recrystallization Textures in Cold Rolled and Annealed (001)[100] Single Crystals of 3% Silicon Iron, *Acta Metall.*, Vol 14, 1966, p 405-423

11. Y. Yoshitomi, K. Iwayama, T. Nagashima, J. Harase, H. Masui, and N. Takahashi, Role of Inhibitor for Secondary Recrystallization Texture Evolution in Fe-3% Si Alloy, *Mater. Sci. Forum*, Vol 113-115, 1993, p 281-286

12. H. Ishitobi and C. Kami, The Formation Process of Forsterite Film in Grain Oriented Si-Fe Sheets, *Current Advances in Materials and Processes - The Iron and Steel Institute of Japan*, Vol 6, 1993, p 1829